

# Multiplicity of detonation regimes in systems with a multi-peaked thermicity. Part 1: Fickett's detonation analogue

Matei I. Radulescu<sup>a</sup>, Justin Tang<sup>a</sup>, Fan Zhang<sup>b</sup>

<sup>a</sup>Department of Mechanical Engineering, University of Ottawa  
Ottawa, Canada

<sup>b</sup> Defence R&D Canada, Suffield, Canada

## 1 Introduction

The decomposition of certain reactive materials can occur in two or more distinct steps, characterized by multiple peaks in the thermicity (effective rate of energy release). Nitromethane-air detonations [1] and other usual fuels using NO<sub>2</sub> as oxidizer [2] give rise to such multiple reaction zone detonation structures. Thermo-nuclear fusion reactions also occur in sequential steps. Detonations in degenerate white dwarfs undergoing Supernova explosion of the Type 1a have three sequential steps as the initial carbon and oxygen matter forms oxygen, silicon and nickel in three sequential steps [3]. Hybrid detonations involving a more reactive gaseous fuel and a less reactive solid reactant also display two sequential reaction zones in the detonation structure [4].

A common feature of multi-peaked thermicity systems is the presence of endothermic processes coupling the multiple reactions. The loss can also be manifested by heat and momentum losses to confining tube walls, or mass divergence and curved geometries. In hybrid systems, for example, the gas phase reaction first proceeds without influence from the solid phase, other than the energy lost to the solid particles to heat them up, and the momentum lost to the solid phase used to entrain the particles with the gas flow. These endothermic processes essentially act as a third much slower reaction that withdraws energy from the gas phase.

It is well known that simultaneous exothermic and endothermic reactions give rise to so-called eigenvalue, or pathological, detonations [5]. The detonation speed is not given by the total energy release, but rather by the energy release evolved until the sonic plane of the detonation, which is located where the rates of energy addition and loss balance, the so-called generalized CJ criterion. It is thus not unreasonable to expect that multi-peaked detonations also have the same character. Nevertheless, two sonic points may be accessible in the same system [4], since the losses may balance the first reaction and/or the second reaction. It is thus not clear which detonation speed will be preferred and what will be the reaction zone structure of such waves.

Experiments in hybrid systems of lean acetylene-air mixtures with micro-metric aluminum powders have indeed revealed a double reaction zone structure with an embedded shock appearing between the

two reaction zones [4]. While the origin of the internal shock was not clear, the observations illustrate the richness of the dynamics of such systems. The present study thus aims to determine the reaction zone structure of such detonations with multi-peaked thermicity.

Our investigation begins with the detonation model introduced by Fickett in the early 1980's [6, 7], which takes the form of the reactive Burger's equation with a reaction source term. The model neglects the rear facing pressure waves of gas dynamics, hence significantly simplifying the mathematical complexity of the description. The model yet retains the important physics of reactive compressible flows and its complex dynamics, namely that pressure waves receive amplification, modulated by the local rate of energy release, and can form shocks [8]. Fickett has already demonstrated how the model can reproduce the complex steady structure of eigenvalue detonations in the presence of one exothermic and one endothermic reaction [7]. The present study addresses the case of a second exothermic reaction, i.e., a system with two peaks of thermicity and an endothermic reaction.

## 2 The model

The Fickett hydrodynamic model is a model for kinematic waves, an extension of the inviscid Burgers' equation to the reactive case. It can be written as:

$$\partial_t \rho + \partial_x p = 0 \quad (1)$$

where  $\rho$  has the meaning of density and  $p$  represents pressure,  $x$  is a Lagrangian coordinate and  $t$  is time. In the present study, we assume the following equation of state:

$$p = \frac{1}{2} (\rho^2 + \lambda_1 Q_1 + \lambda_2 Q_2 - \lambda_3 Q_3) \quad (2)$$

where  $Q_1$  and  $Q_2$  are the energy released by the two reaction steps, and  $Q_3$  is the energy that can be lost. The variables  $\lambda_i$  are the progress variables of each reaction. In the present study, we assume very simple depletion laws:

$$r_1 = \partial_t \lambda_1 = k_1 (1 - \lambda_1)^{\nu_1}, \quad r_2 = \partial_t \lambda_2 = k_2 (1 - \lambda_2)^{\nu_2} (1 - H(1 - \lambda_1)), \quad \text{and} \quad r_3 = \partial_t \lambda_3 = k_3 \quad (3)$$

where all progress variables evolve from 0 in the non-reacted gas to 1. The Heaviside function  $H$  appearing in (3) acts as a switch for the second exothermic reaction, which begins when the first exothermic reaction terminates. The reaction orders are assumed to satisfy the condition  $\nu_i < 1, i = 1, 2$ , such that all reaction zones have a finite spatial extent.

## 3 The structure of self-sustained steady detonations

We seek a traveling wave solution. The initial conditions ahead of the wave are assumed uniform. For simplicity and without loss of generality, we take  $\rho = p = \lambda_1 = \lambda_2 = \lambda_3 = 0$ . The traveling wave solution can be deduced when (1) is written in characteristic form, i.e.,

$$\frac{dp}{dt} = \sigma \quad \text{along} \quad \frac{dx}{dt} = \rho \quad (4)$$

$$(5)$$

where  $\sigma$  is the thermicity

$$\sigma = \frac{1}{2} (r_1 Q_1 + r_2 Q_2 + r_3 Q_3) \quad (6)$$

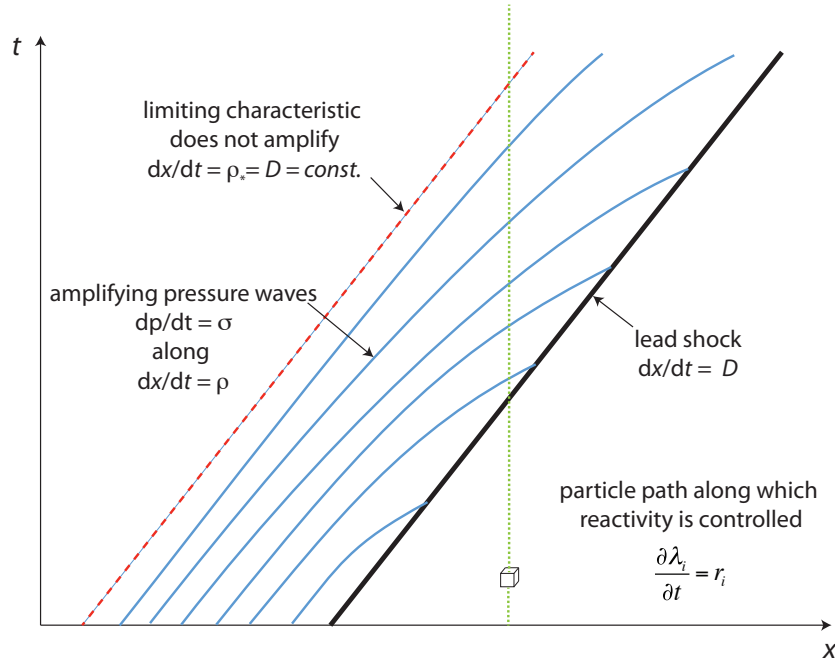


Figure 1: The structure of self-sustained detonations.

Fig. 1 illustrates the structure of the self-supported detonation wave [8]. The detonation structure consists of pressure waves originating from the back, traveling along characteristics  $dx/dt = \rho$  and amplifying according to (4). The amplification is given by the local evolution of the reacting field given by (3) along particle paths  $x = const.$  These pressure waves coalesce and sustain a steady moving lead shock with velocity  $D$ .

The traveling wave solution is isolated from the back when the limiting characteristic travels parallel to the steady lead shock, i.e., when  $dx/dt = \rho_* = D$ . This is the sonic criterion. For this limiting characteristic to travel at constant speed, it also requires vanishing thermicity from (4). Thus the generalized CJ condition, denoted with the subscript \*, becomes

$$\rho_* = D \quad \text{and} \quad \sigma_* = \frac{1}{2} (r_{1*}Q_1 + r_{2*}Q_2 + r_{3*}Q_3) = 0 \quad (7)$$

In order to seek the structure of the traveling wave solution illustrated in Fig. 1, we change the spatial variable to the shock fixed frame, i.e.,  $\zeta = x - Dt$ . For the steady wave solution, we let  $\partial_t = 0$ . We get a single ordinary different equation,

$$\frac{d(p - \rho D)}{d\zeta} = 0 \quad (8)$$

which can be re-written as:

$$\frac{d\rho}{d\zeta} = \frac{1}{D} \frac{\sigma}{\rho - D} \quad (9)$$

Inspection of (9) demonstrates that for a regular solution to exist at a sonic point ( $\rho = D$ ), the thermicity has to simultaneously vanish. This is again the generalized CJ criterion, as demonstrated above using

the limiting characteristic argument. For arbitrary shock speed  $D$ , the general integral curves can be readily obtained by integrating (9) and the reaction rates (3). One obtains

$$\lambda_1 = 1 - \left(1 + \frac{k_1}{D}(1 - \nu_1)\zeta\right)^{\frac{1}{1-\nu_1}} \quad (10)$$

$$\lambda_2 = 1 - \left(1 + \frac{k_2}{D}(1 - \nu_2)\left(\zeta + \frac{D}{k_1(1 - \nu_1)}\right)\right)^{\frac{1}{1-\nu_1}} \quad (11)$$

$$\lambda_3 = -\frac{k_3}{D}\zeta \quad (12)$$

$$\rho = D \pm \sqrt{D^2 - (\lambda_1 Q_1 + \lambda_2 Q_2 - \lambda_3 Q_3)} \quad (13)$$

The solution exhibits sonic points when at any point in the reaction zone,  $\rho = D$ . From (13), we immediately obtain the relation between the detonation speed and the reaction progress variables evaluated along the limiting characteristic:

$$D_*^2 = \lambda_{1*} Q_1 + \lambda_{2*} Q_2 - \lambda_{3*} Q_3 \quad (14)$$

This expression illustrates that the detonation velocity for the solution with sonic points (unsupported) is given by the net energy evolved from the lead shock to the sonic plane.

Further use of the generalized CJ criterion for the balance of rates given by (7) permits to establish the values of the reaction progress variables  $\lambda_{i*}$  along the limiting characteristics. Since the exothermic reactions 1 and 2 are sequential, the balance of rates occurs either between the 1st and 3rd reaction, i.e.,  $r_{1*} Q_1 = r_{3*} Q_3$ , or between the 2nd and 3rd reaction, i.e.,  $r_{2*} Q_2 = r_{3*} Q_3$ . Denoting these two sonic points as sonic points A and B respectively, we obtain the two possible solutions:

$$\lambda_{1*A} = 1 - \left(\frac{k_3 Q_3}{k_1 Q_1}\right)^{1/\nu_1}, \quad \lambda_{2*A} = 0, \quad \text{and} \quad \lambda_{3*A} = \frac{k_3}{k_1(1 - \nu_1)} \left(\frac{k_3 Q_3}{k_1 Q_1}\right)^{(1-\nu_1)/\nu_1} \quad (15)$$

and

$$\lambda_{1*B} = 1, \quad \lambda_{2*B} = 1 - \left(\frac{k_3 Q_3}{k_2 Q_2}\right)^{1/\nu_2}, \quad \text{and} \quad \lambda_{3*B} = \frac{k_3}{k_1(1 - \nu_1)} + \frac{k_3}{k_2(1 - \nu_2)} \left(\frac{k_3 Q_3}{k_2 Q_2}\right)^{(1-\nu_2)/\nu_2} \quad (16)$$

The solution is now complete for the detonation speed and reaction zone structure in closed algebraic forms.

To illustrate the type of solution obtained, let us consider a numerical example with parameters such that  $D_A < D_B$ . Figure 2 shows four families of integral curves for parameters  $k_1 = 1$ ,  $k_2 = 0.2$ ,  $k_3 = 0.1$ ,  $Q_1 = 0.5$ ,  $Q_2 = 0.5$ ,  $Q_3 = 0.8$  and  $\nu_1 = \nu_2 = 0.5$ . For these parameters,  $D_A = 0.59397$  and  $D_B = 0.6$ , while the equilibrium detonation speed is  $D_{eq} = \sqrt{Q_1 + Q_2 - Q_3} = 0.447$ . The integral curves begin at the shock ( $\zeta = 0$ ) with a value of  $\rho$  given by the inert shock jump conditions in Burgers' equation, namely  $\rho = 2D$  and proceed towards the burned side.

For  $D > D_B$ , the integral curve (top most curve in Fig.2) does not intercept any sonic point; this is the overdriven solution, which requires the rear boundary maintained at the corresponding value. The evolution of  $\rho$  is non-monotonous. Initially (zone 1 in Fig. 2),  $r_1 Q_1 > r_3 Q_3$  and the net positive thermicity leads to a positive density (and pressure) gradient, owing to the amplification of forward facing pressure waves. The first zero in density gradient corresponds to when  $r_1 Q_1 = r_3 Q_3$ , the first zero thermicity. Further back (zone 2 in Fig. 2),  $r_1 Q_1 < r_3 Q_3$ , and the density gradient is negative

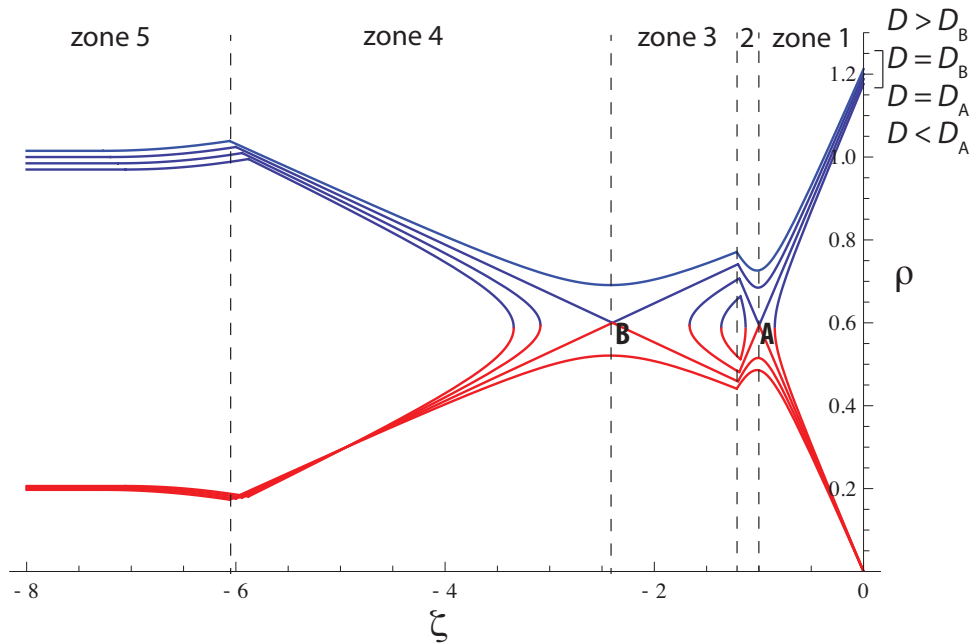


Figure 2: Four families of integral curves; see text for explanations.

as pressure waves are attenuated. Once the second reaction begins and overcomes the endothermic processes (zone 3 in Fig. 2),  $r_2Q_2 > r_3Q_3$  and the density gradient is positive. After the second point of vanishing thermicity obtained when  $r_2Q_2 = r_3Q_3$ , the losses overcome the 2nd exothermic reaction in zone 4 in Fig. 2. The last segment (zone 5 in Fig. 2) corresponds to when the losses are terminated and the second reaction slowly comes to equilibrium.

For a detonation speed corresponding to the largest eigenvalue, i.e.,  $D = D_B$  in this case, a sonic point appears only at the rear (point B), through the balance of the 1st and 3rd reactions. Note that this sonic point is a saddle point, and both weak and strong solutions can be attained in the back, depending on boundary conditions. This is the typical behavior of pathological detonations, and well discussed by Fickett [7]; also see below for the unsteady case.

For  $D = D_A$ , the sonic point occurs at point A, i.e., for the balance between the first and second reaction. Note that however the integral curves corresponding to this solution terminate at a singularity. In the context of an unsteady solution, this signifies that a shock wave will form at the rear, which will eventually catch up to the internal structure all the way to the lead shock. The unsteady solution below illustrates this transient. We can thus assert that the smaller eigenvalue is not stable, but can be established as an intermediate transient.

For detonation speeds lower than both eigenvalues, a steady solution does not exist, owing to the singularity established in the reaction zone, signifying the presence of a strong compression wave in the unsteady case. The equilibrium solution is thus not possible.

Inspection of conditions (15) and (16) for determining the detonation speed eigenvalues (14) reveals the possibility of  $D_A > D_B$ . In this case, the largest eigenvalue,  $D_A$  corresponds to the singularity free solution. The possibility of two sonic points in a steady solution is also possible for a select parameter range such that  $D_A = D_B$ . This solution corresponds to a single integral curve passing through two saddle points.

The solution obtained also admits shock waves anywhere in the reaction zone structure. Since the shock

speed in the Burgers' and Fickett's model is simply given by the average of left and right states, integral curves involving a shock can discontinuously jump between the bottom and top curves, with a negative gradient. Such shocks will travel exactly at the leading shock strength. However, the requirement that a negative gradient be established (forward facing shocks, impossibility of expansion shocks) requires these shocks to be *behind* any sonic point, as only there can a jump from the bottom weak solutions (red curves in Fig. 2) to the strong solutions (blue curves in Fig. 2) occur.

#### 4 Hugoniot and Rayleigh line analysis

The multiplicity of solutions can also be represented in  $\rho - p$  phase space analyzed by traditional Hugoniot-type arguments [6, 7]. Constructing a possible solution requires connecting unburned and burned possible locii (Hugoniots) with possible integral curves (Rayleigh lines) intersecting the locii of zero-thermicity, such as shown in Fig. 2. Such a representation offers further insight into the solution.

For the simple Fickett model considered here, the Hugoniots are simply given by (2) [7]. The non-reacted shock Hugoniot ( $\lambda_1 = \lambda_2 = \lambda_3 = 0$ ), the equilibrium Hugoniot ( $\lambda_1 = \lambda_2 = \lambda_3 = 1$ ), the Hugoniot corresponding to the eigenvalue A, i.e.,  $\lambda_1 = \lambda_{1*B}$ ,  $\lambda_2 = \lambda_{2*B}$ ,  $\lambda_3 = \lambda_{3*B}$  and the Hugoniot corresponding to the eigenvalue B, i.e.,  $\lambda_1 = \lambda_{1*B}$ ,  $\lambda_2 = \lambda_{2*B}$ ,  $\lambda_3 = \lambda_{3*B}$  are shown in Fig. 3 for the numerical example studied in the previous section. Note that the Hugoniot corresponding to the eigenvalue A is slightly lower than that of eigenvalue B for this example.

The integral curves shown in Fig. 2 can also be represented in the  $\rho - p$  phase space of Fig. 3. These form the so-called Rayleigh lines, which, from (8) and boundary conditions at the shock ( $p = 2D^2$ ,  $\rho = 2D$ ) yields a line:

$$p = \rho D \quad (17)$$

Fig. 3 shows these Rayleigh lines for the eigenvalue B and the overdriven solution shown in Fig. 2.

The overdriven integral curve starts at point N, reaches point A on the eigenvalue A Hugoniot, then point B on the eigenvalue B Hugoniot and returns to point S on the equilibrium Hugoniot. Points A and B are the local minima in the corresponding integral curve in Fig. 2, as they correspond to the locus of zero thermicities, as explained above.

The eigenvalue B integral curve shown in Fig. 3 starts at point  $N_{B*}$ , then intersects the Hugoniot A at point  $A_{B*}$  (first zero thermicity point), then proceeds to the sonic point  $B^*$  on the eigenvalue B Hugoniot. Since this point is a saddle point, as shown above, the solution can then reach either the strong solution  $S_{B*}$  or the weak solution  $W_{B*}$ .

The eigenvalue A integral curve (not shown in Fig. 3) is tangent to the Hugoniot A. And since Hugoniot A is lower than B, the corresponding velocity is also lower, via (17). Since this Rayleigh line never intersects Hugoniot B means that a second zero thermicity requirement cannot be established in the system. The detonation speed selection rule and possible steady solution can thus also be made in reference to the Hugoniot analysis. A regular solution requires intersection of the Rayleigh line with both zero thermicity solutions. This can only be achieved for detonation velocities equal or larger than the largest eigenvalue.

#### 5 Shock ignition transient and asymptotic steady states

We have also integrated the unsteady solution predicted by (1) in the framework of a piston driven wave [9]. In order to fully address the richness of the dynamics and complex structure of the wave, we

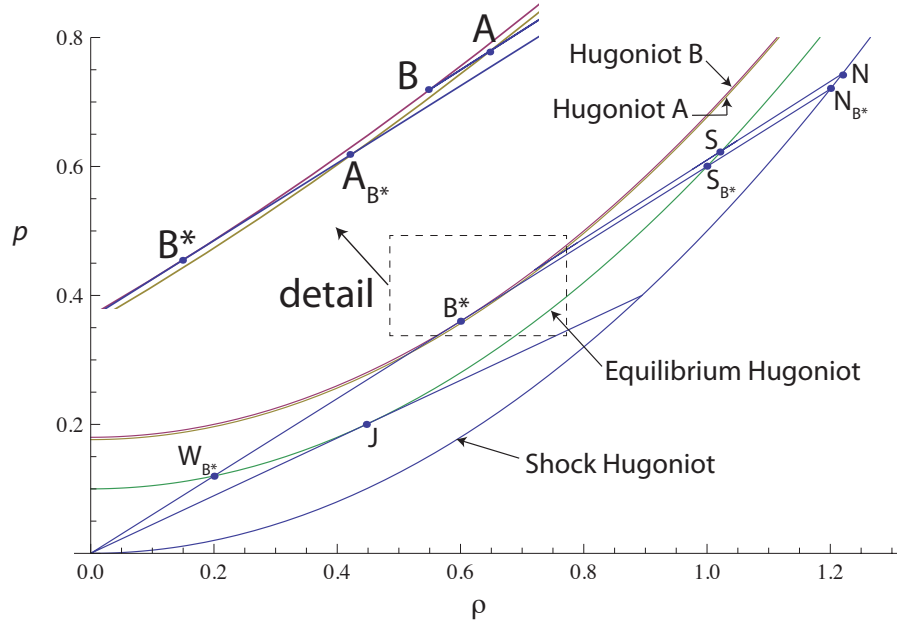


Figure 3: Integral curves on a  $\rho - p$  diagram and Hugoniot curves for the inert shock, equilibrium and the two zero thermicity locii; see text for explanations.

choose a piston speed of  $\rho = 0.35$ , such that the detonation is not supported, and would terminate at a condition slightly larger than the weak solution (see Fig. 2). The details of the numerical technique can be found elsewhere [9]. The parameters used correspond to the case analyzed above.

Figure 4 shows the evolution of the density profiles. The red line shows the evolution of the detonation shock amplitude (i.e.,  $2D$ ). At early times, the solution corresponding to the eigenvalue  $D_A$  is first established. However, a shock appears behind the sonic point A, which travels slightly faster than the main front. Once this shock penetrates through the sonic point A, the entire reaction zone structure rapidly transforms into the steady solution corresponding to  $D = D_B$ , while the shock structure also stabilizes at this value. Comparison with the steady structure obtained for  $D = D_B$  yielded excellent agreement. The unsteady solution thus confirms the structure and selection rules anticipated from the steady structure analysis.

## 6 Conclusions and outlook

Systems with multi-peaked thermicity thus admit multiple steady state solutions. These solutions correspond to the existence of internal limiting characteristics, which isolate the reaction zone structure from rear rarefactions. However, it was shown possible that such solutions may be short-lived for eigenvalues other than the largest ones. For these, the formation of shock waves in the rear, behind the limiting characteristic, can penetrate the reaction zone and modify the reaction structure, until the solution with the largest eigenvalue is established.

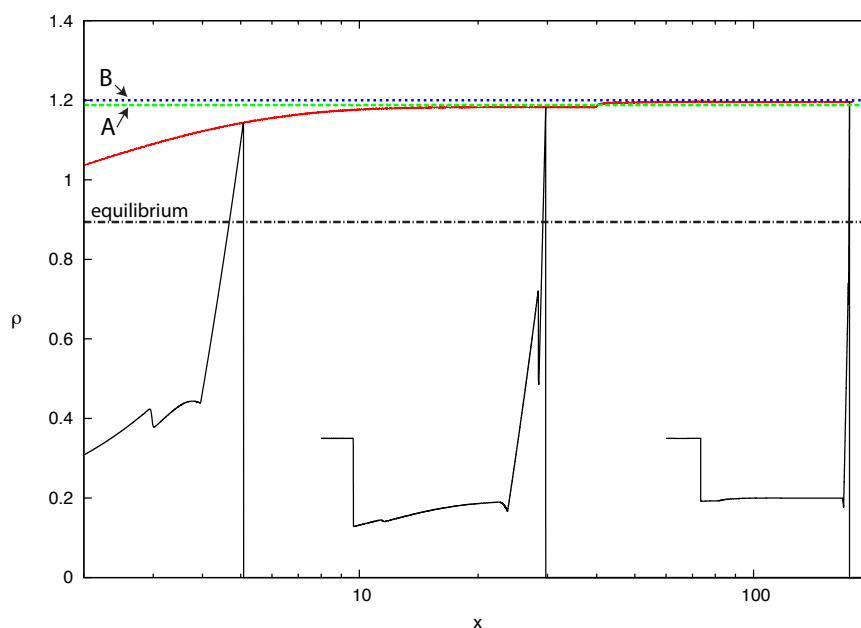


Figure 4: The evolution of the reaction zone structure following shock ignition; same parameters as Fig. 2, illustrating the transition to the smallest eigenvalue, and then to the largest eigenvalue; note the embedded shock behind the reaction zone participating in the transition.

## References

- [1] H. N. Presles, D. Desbordes, M. Guirard, and C. Guerraud, "Gaseous nitromethane and nitromethane-oxygen mixtures: A new detonation structure," *Shock Waves*, vol. 6, no. 2, 1996.
- [2] F. Joubert, D. Desbordes, and H.-N. Presles, "Detonation cellular structure in  $\text{NO}_2/\text{NO}_4$ -fuel gaseous mixtures," *Combustion and Flame*, vol. 152, no. 4, 2008.
- [3] V. N. Gamezo, J. C. Wheeler, A. M. Khokhlov, and E. S. Oran, "Multilevel structure of cellular detonations in type Ia supernovae," *Astrophysical Journal*, vol. 512, no. 2, 1999.
- [4] F. Zhang, "Detonation in reactive solid particle-gas flow," *Journal of Propulsion and Power*, vol. 22, no. 6, 2006.
- [5] W. Fickett and W. C. Davis, *Detonation*, ser. Los Alamos series in basic and applied sciences 1. Berkeley: University of California Press, 1979.
- [6] W. Fickett, "Detonation in miniature," *American Journal of Physics*, vol. 47, no. 12, pp. 1050–1059, 1979.
- [7] ———, *Introduction to detonation theory*, ser. Los Alamos series in basic and applied sciences. Berkeley: University of California Press, 1985.
- [8] M. I. Radulescu and J. Tang, "Nonlinear dynamics of self-sustained supersonic reaction waves: Fickett's detonation analogue," *Physical Review Letters*, vol. 107, no. 16, 2011.

- 
- [9] J. Tang and M. I. Radulescu, “Dynamics of shock induced ignition in fickett’s: influence of  $\chi$ ,” *Proceedings of the Combustion Institute*, vol. 34, pp. 2035–2041, 2013.